Bull. Disas. Prev. Res. Inst., Kyoto Univ., Vol. 34, Part 3, No. 306, September, 1984 

# Seismic Amplification by Soil Deposits Inferred from Vibrational Characteristics of Microseisms

By Junpei AKAMATSU

(Manuscript received June 26, 1984)

**Abstract**

Vibrational characteristics of microseisms as well as of seismic surface waves from near earthquakes were studied to estimate amplification factor due to soil deposits in the Kyoto basin. Around Kyoto microseisms are considered to be surface waves composed mainly of Rayleigh type coming from some specific regions in the Japan sea and the Pacific. The excitation of microseisms depends on the height of sea waves around Japan, in particular on that of the Japan sea coast in winter, and changes with time according to meteorological conditions. Therefore it is indispensable to monitor the wave characteristics of incident microseisms for the sake of seismic microzonation of the basin.

From this standpoint observations of microseisms generated by various weathers such as typhoons, cold fronts and monsoons were carried out at several ground sites in the basin with routine observation at the Sumiyama Seismic Station located on an outcrop of bedrock. The following results are obtained through spectral analyses with automated analogue band pass filtering technique and the Fast Fourier Transform:

Although the spectral characteristics of microseisms such as peak frequency and peak amplitude at the ground site as well as at the rock site change remarkably according to meteorological conditions, the averaged spectral ratio of microseisms at the ground site to that at the rock site shows a frequency dependent constant shape, which is considered to be an amplification factor of microseisms due to soil deposits. The reliability of the estimated amplification can be checked with a standard deviation as long as the observations with a recording length of longer than 4 minutes are repeated at least 6 times. Amplification in the horizontal component begins to increase at lower frequencies than that in the vertical one. The horizontal component has larger peak amplification than the vertical one. The frequency of peak amplification and critical frequency at which amplification begins to increase become lower as an observational ground site moves from the environs to the center of the basin. The variation of amplification with component and site location is interpreted to be attributable to the mode conversion of incident surface waves at the boundary of the basin and to the resultant interference between modes in the basin. Amplification of seismic surface waves derived from spectral ratios of near earthquakes resembles that of microseisms very well. Therefore microseismic study is useful for direct measurement of seismic amplification due to soil deposits in the frequency range of lower than about 1 Hz.

## 1. Introduction

Vibrational characteristics of microtremors with periods of longer than 1 second at ground sites have been studied in the interest of finding an applicability to the problems in engineering seismology[1-3]. Predominant periods and amplitudes of tremors are examined in relation to such a deep geological structure that the depth of bedrock is over 100 meters[1-3]. Appearance of spectral peaks of the tremors at a ground site depends on the velocity contrast between soil deposits and bedrock[3]. It is well known that microtremors with this period are microseisms caused mainly

by sea waves, and that both period and amplitude change extremely depending on a meteorological condition in and around Japan[4,5]. Thus, when microseismic observation is carried out in a wide area for the sake of seismic microzonation, it is indispensable to monitor the wave characteristics of incident microseisms. In the case in which the objective area has a long coast or lies near sea, the problem is complicated, because the area is near the source region of microseismic waves[6]. Contrarily, in inland areas such as the Kyoto basin, it is expected to be able to estimate the amplification factor of surface waves due to soil deposits with comparative observations at ground and rock sites, because the microseisms are considered to be composed mainly of Rayleigh waves coming from the far regions. However, there are another problems related to mode conversion of incident surface waves at the boundary of the basin and interference of modes[7].

Fortunately the nature of stormy microseisms, such as wave type, condition of generation and source region, were investigated critically around Kyoto[8,9], and the subsurface structure in the southern parts of the Kyoto basin has been studied with geophysical prospecting[10]. From this standpoint observations of microseisms generated by various meteorological conditions were carried out at several ground sites including the Seismological Station of the Disaster Prevention Research Institute of Kyoto University at Uji (INST) in the Kyoto basin, with routine observation at the Sumiyama Seismic Station (SUM) located on an adjacent outcrop of Paleozoic strata for monitoring the characteristics of incident microseisms. We also examined the vibrational characteristics of seismic surface waves from near earthquakes with use of the data at SUM and INST. Some of the results such as temporal variation of microseisms, amplification of microseisms due to soil deposits, relation between amplification and geological setting, and the problem in observation, have been reported in a previous paper[11]. In addition, we discuss the amplification of seismic surface waves from near earthquakes, relation of amplifications between microseisms and seismic surface waves, and related problem to microseismic observation for seismic microzonation.

## 2. Some general features of microseisms around Kyoto

Microseisms are markedly excited when a typhoon is passing near Japan or when monsoons blow hard in winter. Okano critically studied the nature of stormy microseisms observed under various meteorological conditions such as typhoons, cold fronts and monsoons[8,9]. Some important results are as follows: microseismic waves are of Rayleigh type generated by swell in the region of the Japan sea off the Tango peninsula and that of the Pacific off the Kii peninsula; the period is 2–7 sec and amplitude exceeds 5 $\mu$m in the largest case; the amplitude is larger for the longer period; the wave velocity is approximately 3.0 km/sec for a period of 4 sec.

A short period seismometer system, operating at SUM[12], often records such stormy microseisms, the apparent period of which is 2–4 sec as seen in **Photo 1.**

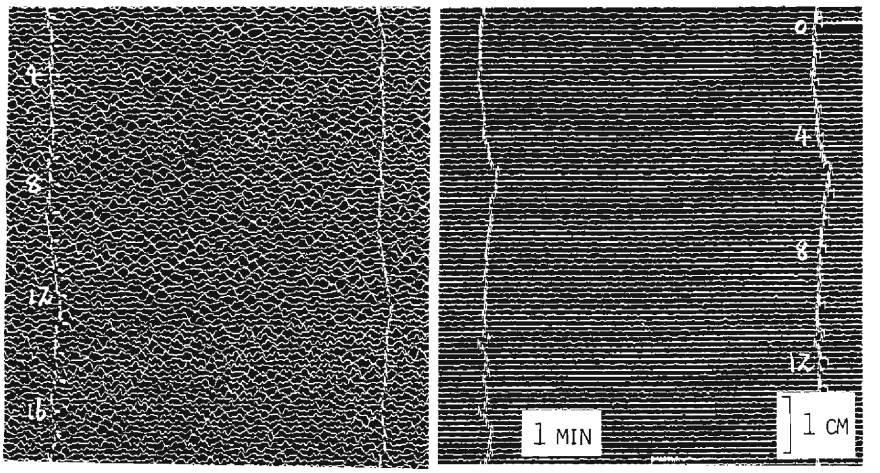


(A) (B)

Photo 1 Examples of microseisms recorded on smoked paper operating at the Sumiyama Seismic Station (SUM) for seismic monitoring. (A): excited microseisms on Feb. 17 1981, (B): calm microseisms on Feb. 15 1981

There is a marked contrast between such stormy microseisms and artificial microtremors with periods shorter than about 1 sec observed usually in calm weather. **Fig. 1** shows the relation between the amplitude of microseisms on the smoked paper and the height of significant sea waves along the Japan sea coast[13]. Sensibility of the recording system decreases rapidly in the frequency range of microseisms, that is, lower than 1 Hz (cf. **Fig. 3**). The observational point of sea waves is the Tottori Harbor and is separated by 100 km from the coast of Kyoto prefecture. In spite of these unfavourable conditions, a good, positive correlation is obvious. When the height of significant sea waves is over 1 m, microseisms are observed directly with the usual short period seismometer.

## 3. Observation and analysis of microseisms

### 3.1. Observational points

Microseismic observations were carried out in the southern parts of the Kyoto basin and on the adjacent outcrop of the Paleozoic strata. The observational points and rough geological map are shown in **Fig. 2**. The basin is surrounded by the late Paleozoic complex consisting mainly of sandstone, slate and chart. The soil deposits are the Plio-Pleistocene Osaka Group with thin alluvial deposits and lie on the late Paleozoic basement. In the south-eastern margin of the basin the Osaka Group forms mountain gravels and terraces. The seismic refraction investigation, carried out along an east-west line passing GOK and OGR, gives a two layer velocity model: the soil layer with a velocity of 2.0–2.1 km/sec and the basement layer with a velocity of 4.4–5.2 km/sec; the configuration of the basmeent layer is shaped like

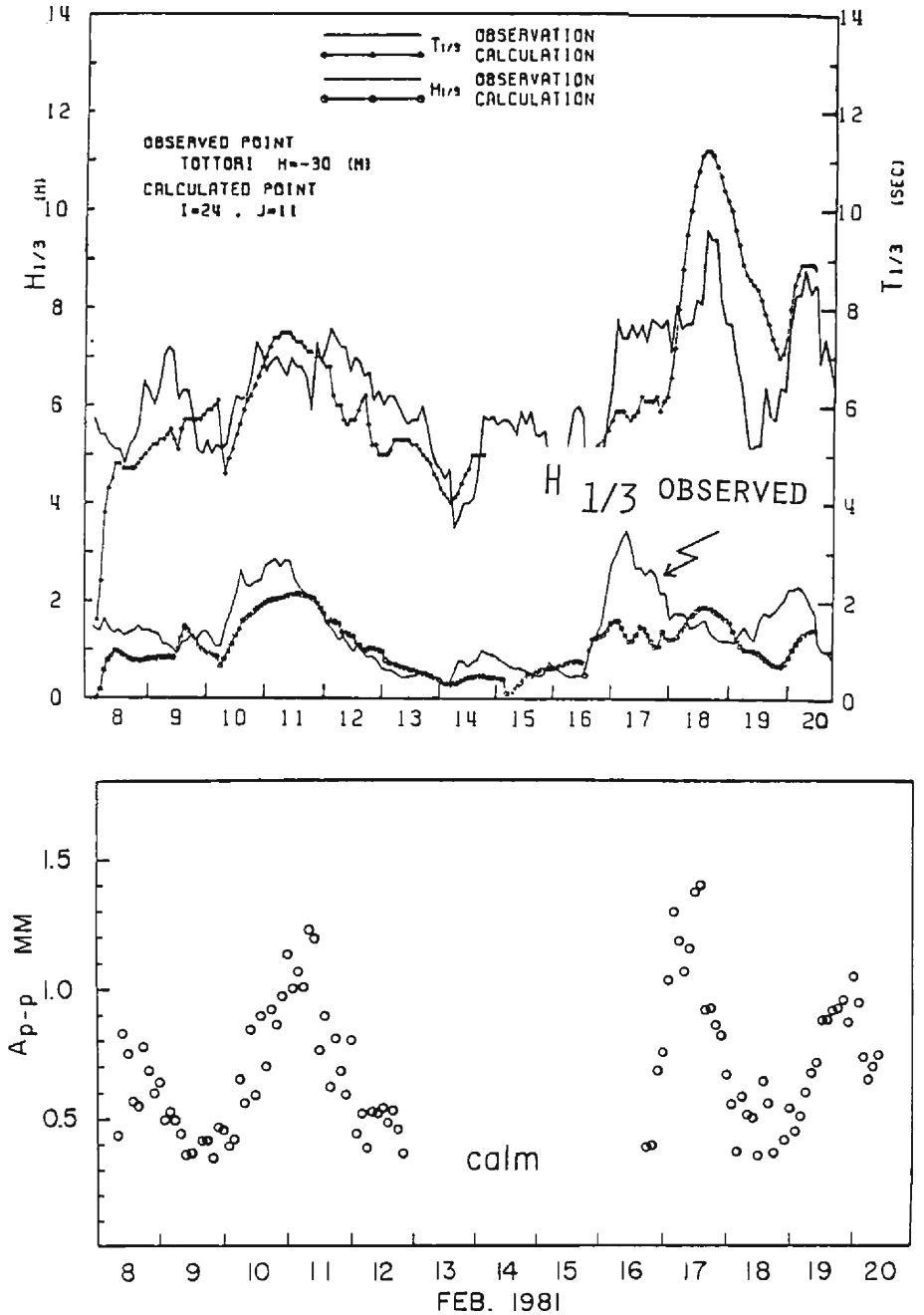


Fig. 1 Comparison of microseisms at SUM with sea waves along the Japan sea coast. Amplitude of microseisms is an averaged value of the five largest peak-to-peak amplitude in 2 minute intervals at every 2 hours on the smoked paper. The figure of the sea waves at Tottori Harbor is reproduced from **Fig. 14** of Tsuchiya et al (1983)[13]. Note that excellent positive correlation exists between excitation of microseisms and height of significant sea waves, $H_{1/3}$.

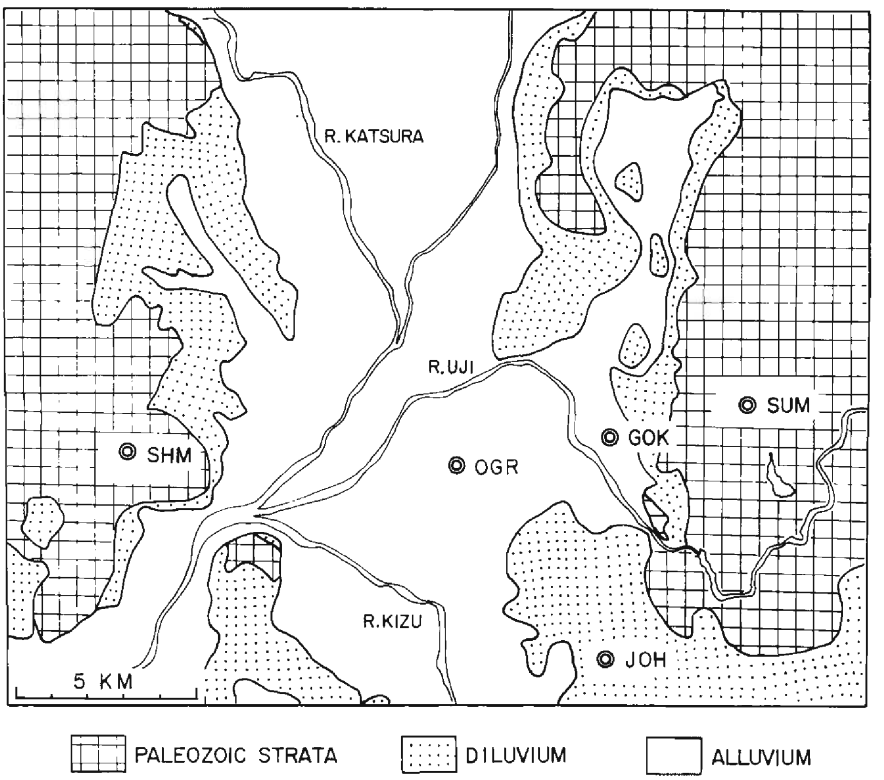


Fig. 2 Rough geological map of the southern parts of the Kyoto basin and locations of observational points

a ship bottom; the depth of basement layer is approximately 700 m at OGR and 370 m at GOK[10,14].

The Seismological Station in the main building of the Institute (INST) is situated at GOK. SUM is the Sumiyama Seismic Station based on an outcrop of Paleozoic strata, the velocity of which is 4.66 km/sec for P wave and 2.58 km/sec for S wave to a depth of about 1 km[15].

The temporary stations OGR, JOH and SHM were set up on the typical geological setting. OGR is situated on a reclaimed land of the Ogura-ike pond in the center of the basin, where the basement is estimated to be deepest. JOH is on mountain gravels with a thickness of more than 50 m. In order to examine the uniformity of incident microseisms to the whole basin, SHM was set on an outcrop of Paleozoic strata on the west end of the basin in the opposite direction to SUM.

### 3.2. Observational time

The observational times at each station are listed in **Table 1**. In the time No. 1, the typhoon 8122 passed north-east along the Japan islands on the Pacific and weakened near the Kamchatka peninsula. The predominant frequency of microseisms excited by the typhoon on the Pacific was lower than 0.15 Hz. After a day,

Table 1 List of observational times and causes of stormy microseisms

| No. | Station | Observational time | Condition |
|---|---|---|---|
| 1 | SUM | Sep. 24 13h—Oct. 8 11h '81 | Typhoon 8122 |
| | GOK | Oct. 3 20h—Oct. 7 10h | and cold front |
| 2 | SUM | Dec. 31 14h—Jan. 11 3h '82 | cyclones and |
| | GOK | Dec. 31 18h—Jan. 9 9h | monsoon |
| 3 | SUM | Sep. 22 13h—Oct. 1 11h '82 | Typhoon 8219 |
| | GOK | Sep. 22 21h—Sep. 30 16h | |
| 4 | SUM | Dec. 30 13h—Jan. 3 7h '83 | monsoon |
| | GOK | Dec. 30 11h—Jan. 3 12h | |
| 5 | SUM | Mar. 2 12h—Mar. 6 9h '83 | |
| | GOK | Mar. 2 13h—Mar. 6 16h | cyclone |
| | OGR | Mar. 2 19h—Mar. 3 6h | and |
| | SHM | Mar. 3 19h—Mar. 4 6h | monsoon |
| | JOH | Mar. 4 18h—Mar. 5 6h | |

a cold front passed over the Japan sea. The predominant frequency was 0.3–0.4 Hz. The difference in the predominant frequency is attributable to the difference between the preiod of swells in the Pacific and that in the Japan sea. All these natural occurrences have been discussed in the previous paper[11].

In the observational time No. 3 the typhoon 8219 passed across the Shikoku and Chugoku districts of the western Japan and went north-east over the Japan sea (Fig. 9). Microseisms were exicted markedly before noon on October 25, when the typhoon passed through the area off Kyoto prefecture.

During the times Nos. 2, 4 and 5 microseisms grew high and low according to meteorological conditions such as cyclone, cold front or monsoon.

### 3.3. Method of observation and analysis

As seen with an example in **Photo 1** stormy microseisms at a rock site can be observed with a usual short period seismometer consisting of 1–sec geophone and D.C. amplifier with a good signal to noise ratio and accuracy. However, when an observation is carried out on a ground site with the same instrument, the signal will be clipped owing to a high frequency component in artificial tremors generated in the urban area. Thus we used an integrator circuit to decrease the high frequency component at the ground site as shown in **Fig. 3**. The output signal of the geophone or the integrator circuit was amplified 5,000 or 10,000 times and was recorded by FM data recorder, which was driven automatically for 2 or 4 minutes on every hour. The total record files amount to more than 1,600 items.

In order to examine the frequency contents and their temporal variation, we developed a hybrid technique for easy estimation of spectrum using a digital microcomputer system with A/D and D/A converters and three analogue band pass filters (B.P.F.). The procedure is shown in **Fig. 4**. Though the center frequencies of

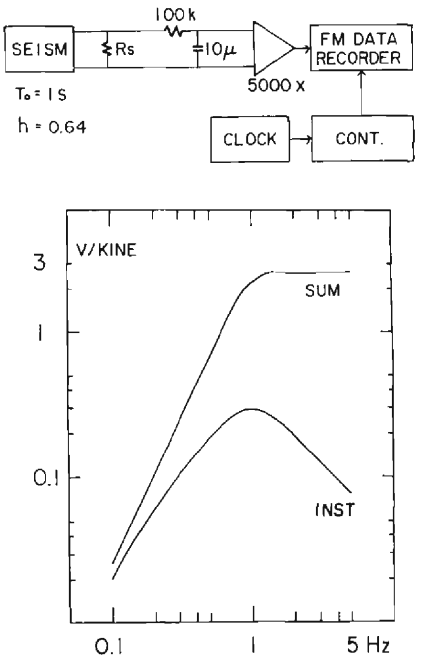


Fig. 3 Observational system of microseisms and frequency response of geophone

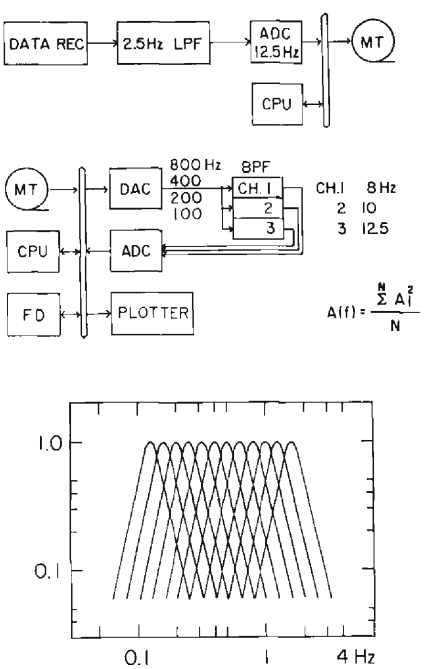


Fig. 4 Procedure of analysis and reusltant response of band pass filters

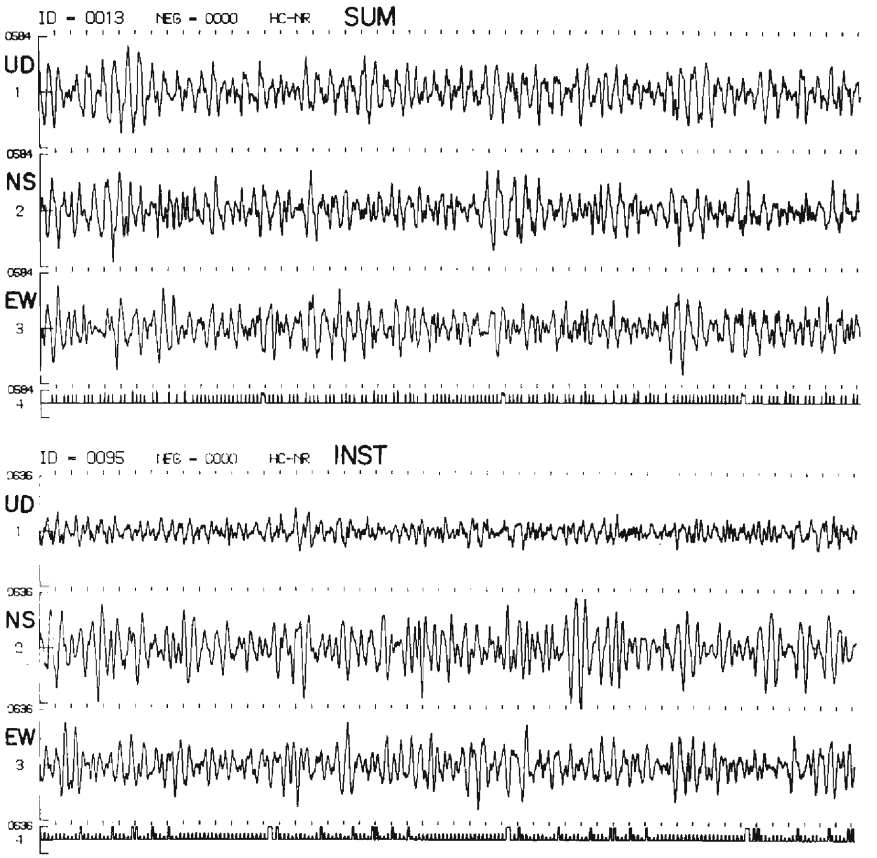


Fig. 5 An example of microseisms analyzed, Fourier spectra of which are shown in Fig. 16

B.P.F. are set manually to be 8, 10 and 12.5 Hz at the beginning of analysis, they change apparently into different frequency bands depending on the relation between the sampling rate of the original data (12.5 samples/sec) and the clock rate of D/A converter (800, 400, 200 and 100 Hz) which produces input signal to B.P.F. As a result we obtain 12 pass bands from 0.13 to 1.6 Hz with 1/3 octave step. Thus we obtained a pseudo power spectrum, with giving an instrumental correction to the mean squared amplitude of B.P.F.

**Fig. 5** shows an example of original digital data of microseisms. It should be noticed that the amplitudes of three components at the rock site, SUM, are nearly same, but that the amplitudes of the horizontal components are larger than that of vertical one at the ground site, GOK (INST).

## 4. Observation and analysis of seismic waves

We intended to discuss the amplification of seismic surface waves due to soil deposits in connection with the problem of microseisms. For the rock site, SUM,

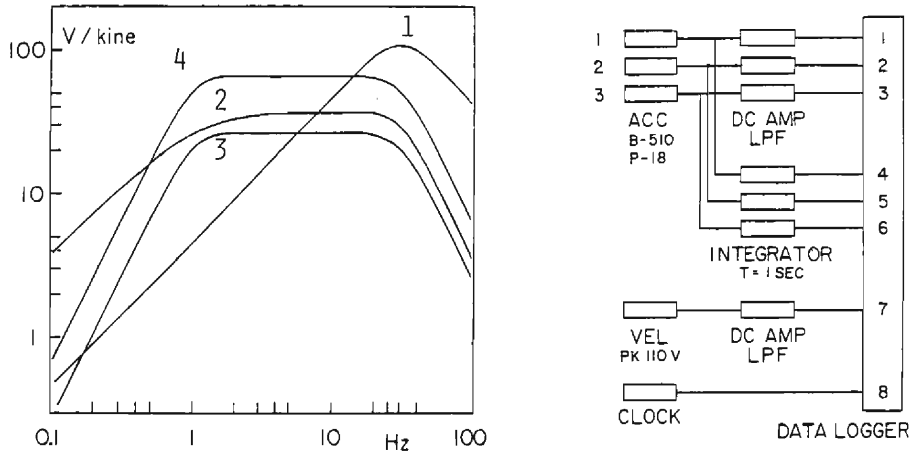


Fig. 6 Observational system of seismic waves at the Institute and frequency response. (1): CHS. 1, 2, 3. (2): CHS. 4, 5, 6. (3): CH. 7. (4): system at SUM

Table 2 List of the events analyzed

| No. | Code | Time | | Date | | | Lat | | Lon | | Azim | R | H | M |
|---|---|---|---|---|---|---|---|---|---|---|---|---|---|---|
| | | h | m | m | d | y | d | m | d | m | d | km | km | |
| 1 | SUM–312 | 12 | 48 | 08 | 08 | 83 | 35 | 31.1 | 139 | 01.5 | 76 | 297 | 22 | 6.0 |
| 2 | SUM–352 | 05 | 24 | 08 | 26 | 83 | 33 | 33.2 | 131 | 36.4 | −110 | 419 | 116 | 6.8 |
| 3 | SUM–449 | 22 | 34 | 10 | 03 | 83 | 34 | 0.2 | 139 | 30.9 | 106 | 352 | 15 | 6.2 |
| 4 | SUM–503 | 01 | 52 | 10 | 31 | 83 | 35 | 24.8 | 133 | 55.6 | −72 | 183 | 15 | 6.2 |
| 5 | SUM–503' | 01 | 55 | 10 | 31 | 83 | 35 | 26.2 | 133 | 59.5 | −71 | 179 | 13 | 5.7 |

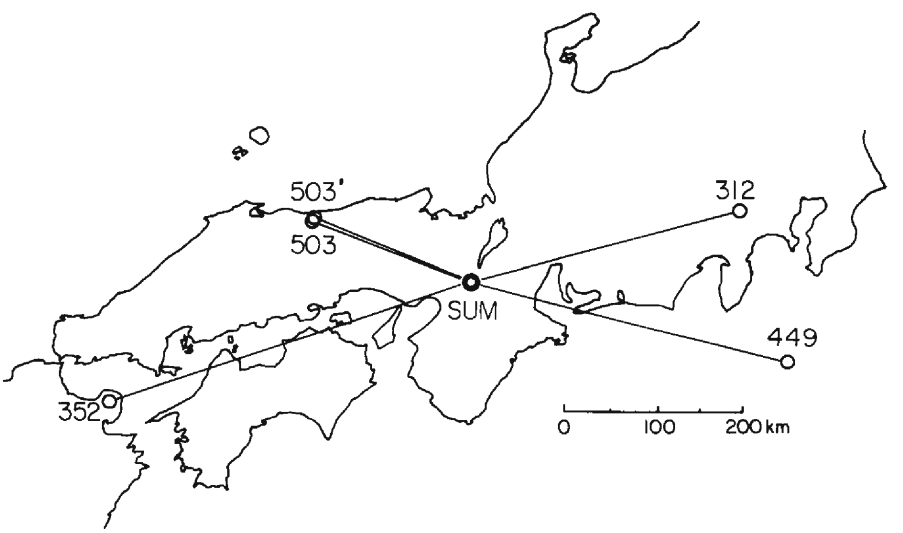


Fig. 7 Locations of the events used for surface waves analysis

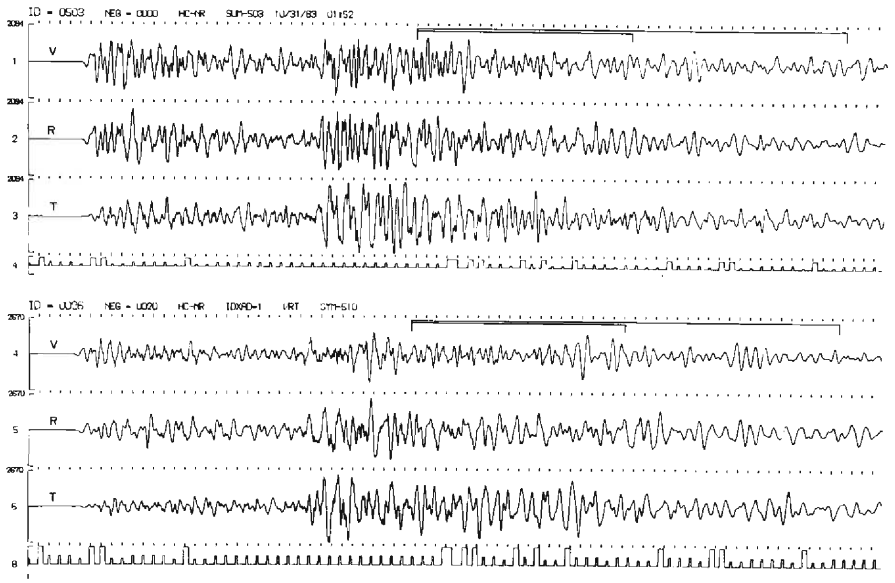

Fig. 8 An example of 3 component seismograms. The horizontal components are rotated to the radial and transversal ones for the source azimuth. The time windows for Fourier spectral analysis are indicated in the upper parts of the vartical components. Oct. 31, 1983, 01h 52m, R=183.4 km.

we used the analogue magnetic records, obtained routinely by the symmetrical seismograph system[16]. The digital magnetic data with a system in **Fig. 6** were available for the ground site, GOK (INST). The events analyzed are listed in **Table 2**. The epicenters reported by the Japan Meteorological Agency (J.M.A.) are plotted in **Fig. 7**. **Fig. 8** shows an example of 3 component seismograms, the horizontal components of which are rotated to the radial and transversal components for the source azimuth. We discuss the Fourier spectra of the surface waves in the window of 20.5 sec or 41 sec immeadiately after the S wave group as indicated in **Fig. 8**.

## 5. Result and discussion

### 5.1. Temporal variation of spectra and spectral ratio for microseisms

The spectra of microseisms at a ground site as well as a rock site vary with time both in peak frequency and in peak amplitude according to the meteorological condition in the observational times from No. 1 to No. 5. However, the spectral ratio, which is considered as a ground response to microseism, has no significant variation regardless of the frequency content of any microseism. This matter is argued critically with an example of analysis for typhoon 8122 in a previous paper[11]. We can see two examples in the following.

**(1) Stormy microseisms excited by typhoon 8219**

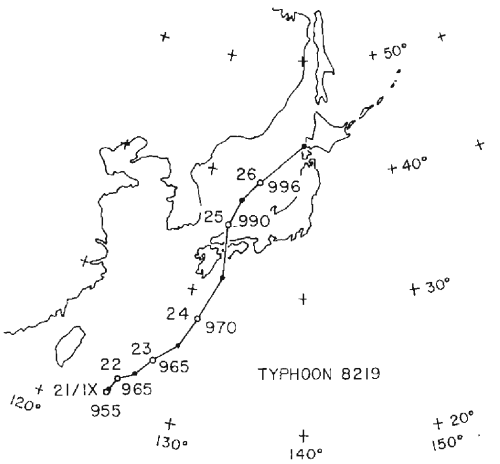


Fig. 9 Travelling path of typhoon 8219. Open and closed circles denote the locations at 9 and 21 o'clock, respectively.

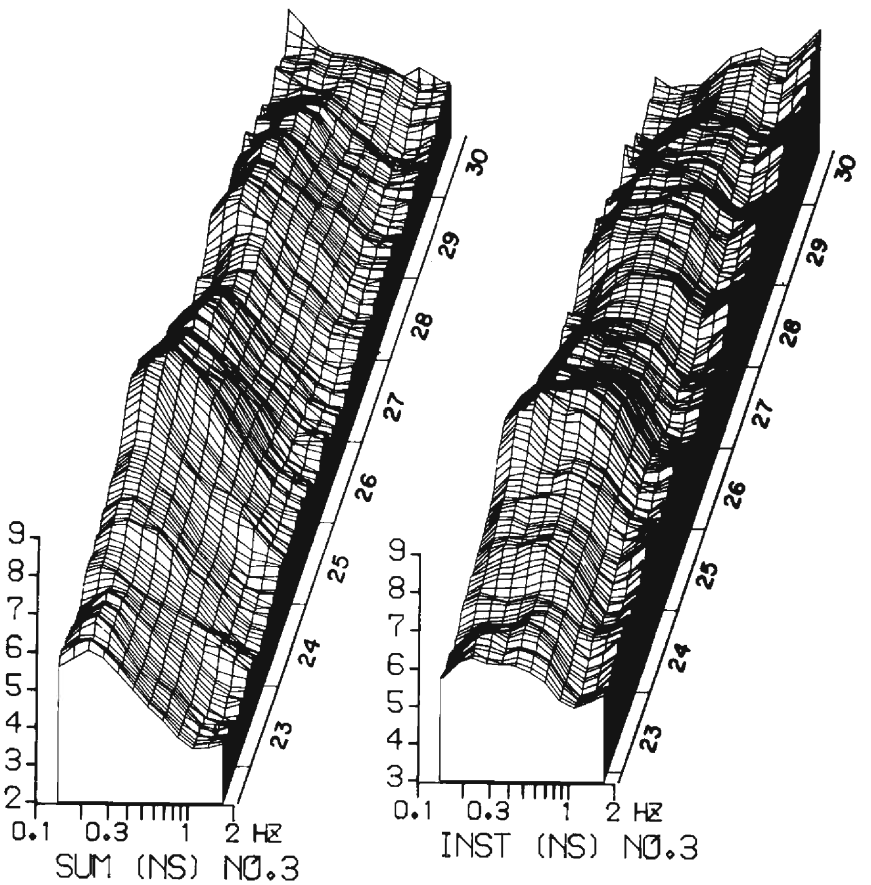


Fig. 10 Variation of amplitude spectra of microseisms caused by typhoon 8219. Amplitude scale is an arbitrary logarithmic unit.

The typhoon 8219 passed across the Chugoku district to the Japan sea on September 25 1982, and went north-east as shown with the travelling path in **Fig. 9**. The variation of spectra in the horizontal component is displayed with a three dimensional graph in **Fig. 10**. The ordinate is arbitrarily scaled by the common logarithms of the mean squared amplitude. The spectra at the rock site, SUM, have a rather simple shape with a peak around 0.2 Hz. Contrarily, the spectral shape at the ground site, INST, is complicated with additional peaks from 0.3 to 0.7 Hz. Before noon on September 25 the amplitude increased to its highest level and the peak frequency became lowest at each site in the same way. The appearance of the 0.3–0.7 Hz peaks at INST corresponds to that of lobes on the side slope at SUM. The diurnal change is obvious in the higher frequency range than about 1 Hz, in which artificial microtremors are predominant.

In **Fig. 11** the temporal variation in some typical bands is drawn up for detailed comparison between the two sites. In the 0.2–0.25 Hz band the amplitudes at SUM and INST are almost always same and vary with time in parallel. In the 0.4–0.5 Hz band, although there is a large difference between the amplitude levels, the parallel variation is conspicuously kept. This can be seen in the simultaneous appearances of the 0.3–0.7 Hz peaks at INST with that of lobes at SUM as pointed in **Fig. 10**. Thus there can be a linear relation of amplitude at the ground site with that at the rock site regardless of the amplitude levels. In particular the 0.4–0.5 Hz component at the ground site, which often forms a spectral peak beside the 0.2–0.25 Hz peak of incident microseisms, makes a peak, not without relation to,

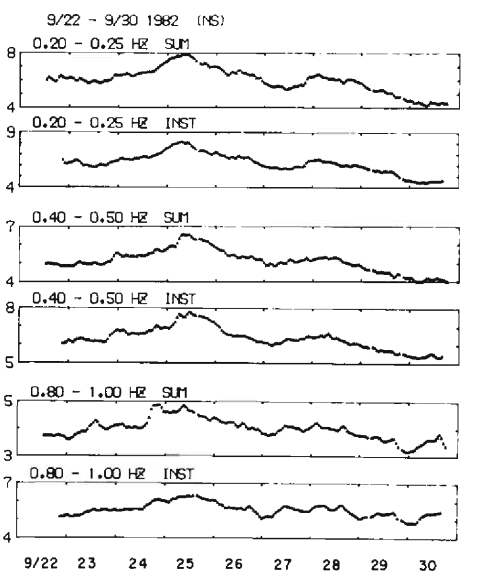


Fig. 11 Comparison of the amplitude variation with time at the rock site, SUM, and the ground site, GOK (INST)

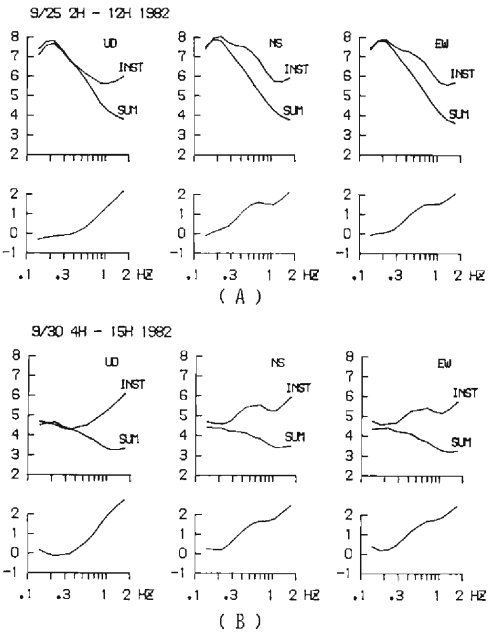


Fig. 12 Averaged spectra and spectral ratio (INST/SUM) of microseisms, (A): excited remarkably by typhoon 8219, (B): after the typhoon. Though spectral shapes are different with time, spectral ratios have the same feature.

but with a linear relation to the same frequency component at the rock site. In the higher frequency range of 0.8–1.0 Hz, the artificial tremors generated locally in the urban area affect and weaken the linear relation.

**Fig. 12** shows the typical averaged spectra and the ratio of the spectra at the ground site to that at the rock site. At the rock site, SUM, the spectral shapes of the horizontal components are same as that of the vertical one. Contrarily, at the ground site there is a remarkable difference between the horizontal components and vertical one in the frequency range of 0.3–0.8 Hz. This is observed clearly in the spectral ratio. That is, in the vertical component the ratio is nearly one below 0.3 Hz and increases with frequency up to 30–40 at 1 Hz. In the horizontal components the ratios begin to increase at 0.2 Hz and make rough peaks at 0.7 Hz and troughs at 1 Hz. These features of spectral ratios are commonly observed. However, when the microseisms are calm, the troughs around 1 Hz are weakened by the artificial tremors.

### (2) Microseisms caused by monsoon in winter

The feature of microseisms observed frequently in winter is common to that of the stormy microseisms caused by typhoons in the sense of the amplification effect due to soil deposits. In the observational time No. 2 the microseisms varied with time as shown in **Fig. 13**. In this period, high atmospheric pressures and low pres-

sure troughs with cold fronts moved from the China continent to the Pacific, one after the other. The weather charts are shown in **Fig. 14**. The amplitude was of the lowest level during the period from 15 o'clock Jan. 3 to 15 o'clock Jan. 4, in which the wide area around Japan was covered by a high pressure. **Fig. 15** shows the typical averaged spectra and their ratios of the excited and calm microseisms, from

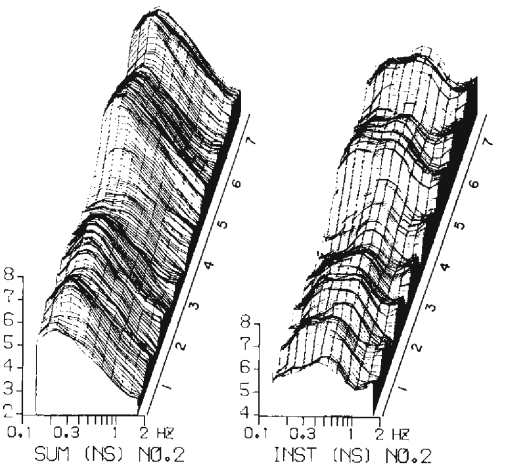


Fig. 13 Variation of amplitude spectra of microseisms in the observational time No. 2 in winter

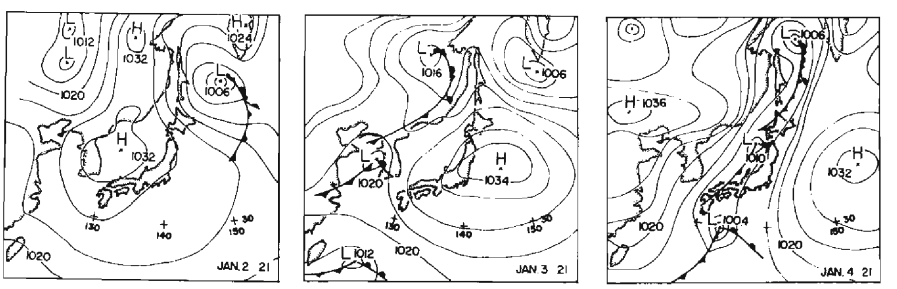


Fig. 14 Weather charts in the observational time No. 2 in 1982

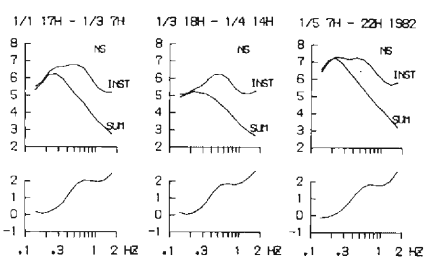


Fig. 15 Averaged spectra and spectral ratios (INST/SUM) of microseisms under different weather conditions as shown in Fig. 14

which we can obtain the same result of amplification due to soil deposits as that of the stormy microseisms (cf. **Fig. 12**). It is favourable for microseismic observations that the amplitude level is high enough to examine the spectral ratio even under calm weather in winter.

### 5.2. Fourier spectra of microseisms and seismic surface waves

The above discussion is based on the result of B.P.F. analysis. We will discuss the Fourier spectra for reexamination of the frequency contents with increased frequency resolution and for the absolute value of spectral density, which will be important in the temporal observation for seismic microzonation.

The results are shown in **Fig. 16**. The Fourier spectral densities in **Fig. 16(a)** are obtained from the records in **Fig. 5** with a window of 164 sec by the F.F.T. and the Hunning smoothing processing. In this example there are peaks at 0.2 and 0.3 Hz in the lower frequency range both at the ground and rock sites. At the ground site each horizontal component has an additional large peak at 0.38 Hz. These peaks with such a narrow width cannot be identified by the B.P.F. analysis. **Fig. 16(b)** shows spectral ratios, in which six results are plotted. Although there are many peaks and troughs in the ratios, we cannot find a significant peak which is commonly observed in each ratio, but can see rough peaks around 0.7 Hz in each horizontal component. The appearance of many peaks and troughs is due to the statistical characteristics in the F.F.T. The means of the ratios in **Fig. 16(c)** rule out the meaningless peaks and troughs and show the similar frequency dependent natures to those of the ratios by the B.P.F. analysis as shown in **Figs. 12** and **15**. The ratios of the horizontal components in **Fig. 16(c)** have rather rapid increase from 0.3 to 0.38 Hz and more remarkable troughs at 1 Hz than the spectral ratios by the B.P.F. analysis. This is due to the difference in the ability of frequency resolution between the Fourier analysis and the analogue B.P.F.

**Fig. 17** shows the results of seismic surface waves. The spectra (**a**) and spectral ratios (**b**) are obtained from the seismograms shown in **Fig. 8** with a window of 41 sec. In the ratios (**b**), there are peaks at 0.38 and 0.63 Hz in the radial component, and at 0.35 and 0.7–0.8 Hz in the transversal component. The amplification is approximately 2.5 in each lower frequency peak and is 8–10 in each higher frequency peak. The peak frequency and peak amplitude in the ratios change from event to event as seen in the figure (**c**), which includes 5 results of the events listed in **Table 2**. One of the reasons for this change with event is attributable to the difference in mode contents of incident surface waves and in path effect, because the source depth and the crustal structure will affect the excitation of surface waves. It is also cited for an another reason, that the incident surface waves suffer from the mode conversion at the boundary of the basin and that the interference of modes occurs in the basin[7]. Amplitudes in the basin are modulated and vary with distance from the boundary. Since the distance between the observational ground site and the boundary varies according to source azimuth, the effect of intereference can appear in a

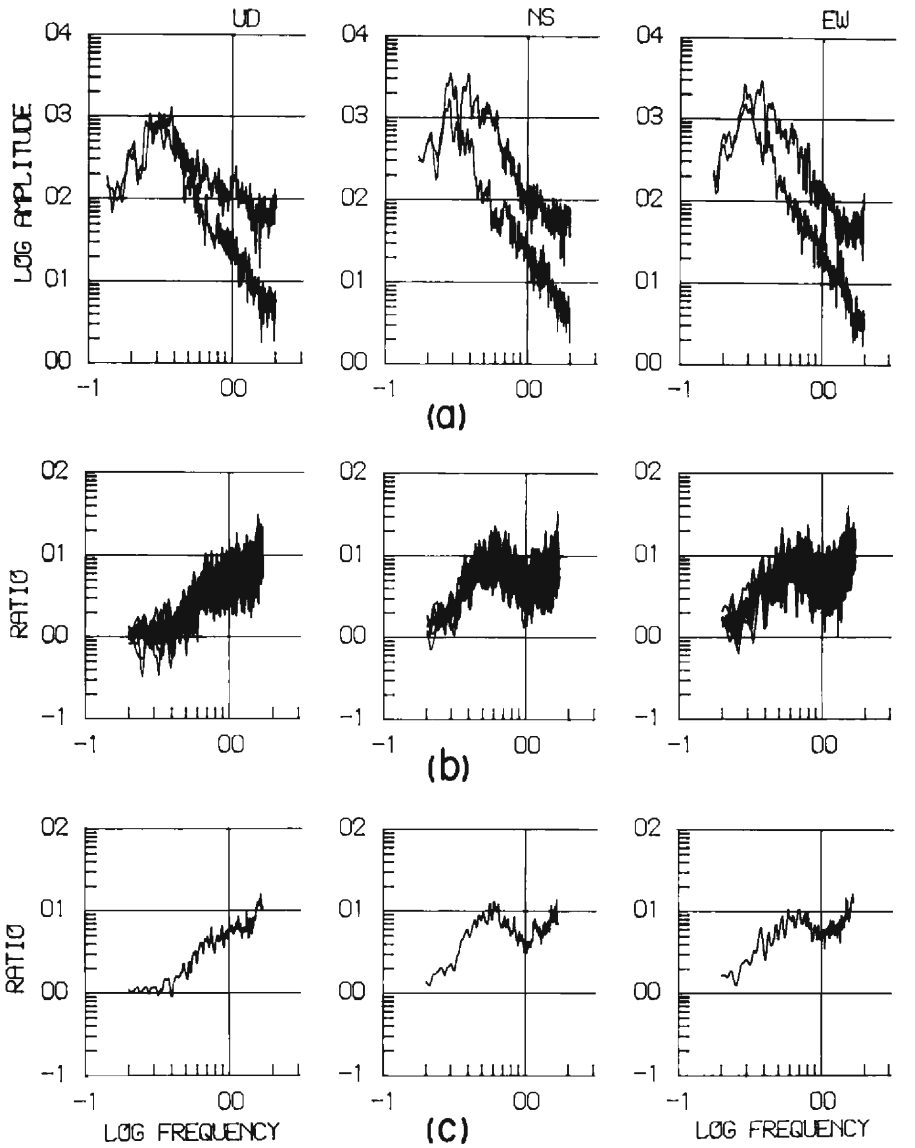


Fig. 16 An example of Fourier spectral analysis of microseisms. (a): Comparison of Fourier spectral densities at SUM and INST. Microseisms analyzed are shown in Fig. 5. Amplitude scale is in $\mu$ kine sec. (b): Spectral ratios. Six results are plotted simultaneously. (c): Averaged spectral ratio.

different manner from even to event.

The averaged spectral ratios in **Fig. 17(d)** have the similar frequency dependent characteristics to those of microseisms in **Fig. 16(c)** both in the horizontal and vertical components. It can be noted that the peak amplification of each event is nearly same as the averaged spectral ratios of microseisms. In spite of the difference

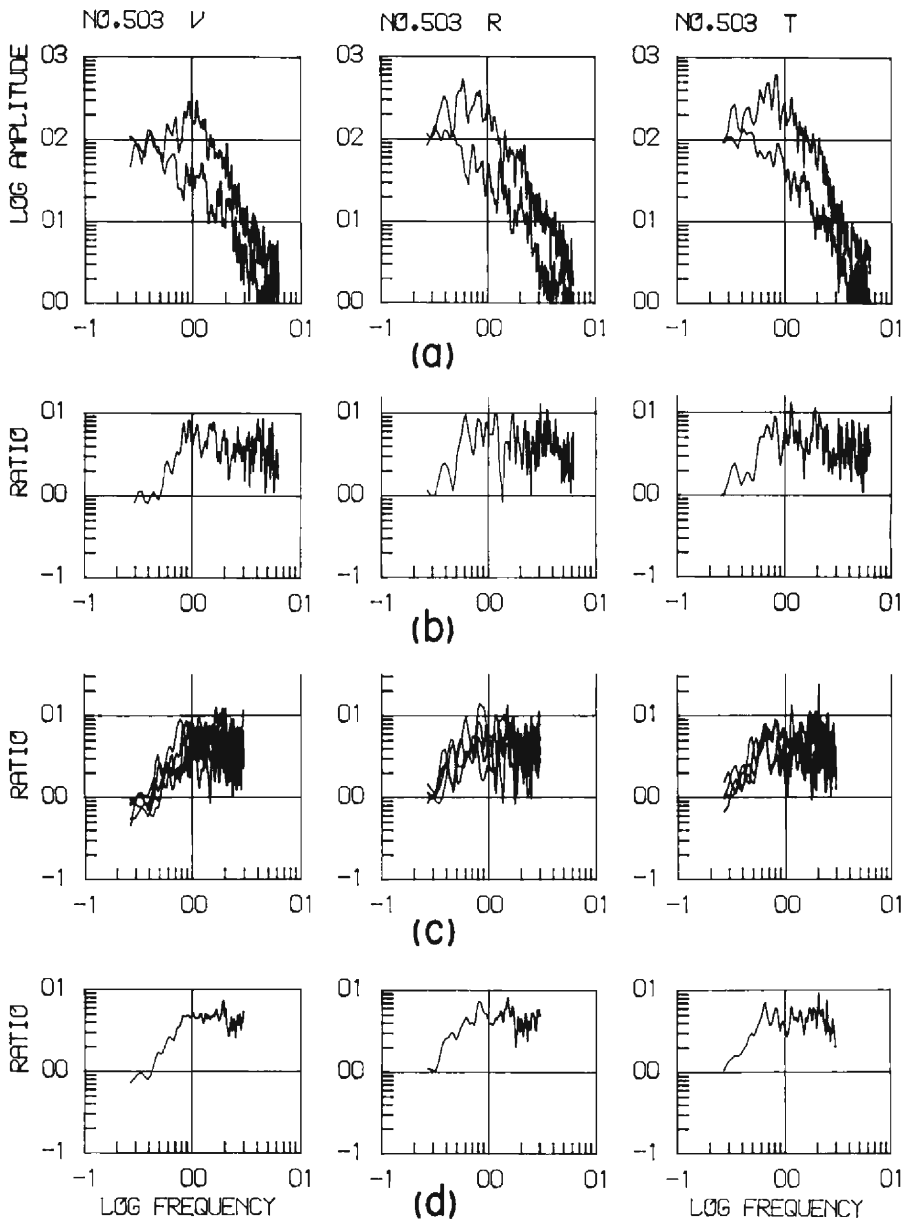


Fig. 17 Results of Fourier spectral analysis of seismic surface waves with 41 sec time window. (a): Comparison of Fourier spectral densities. The seismic waves analyzed are shown in Fig. 8. Amplitude scale is in m kine sec. (b): Spectral ratio (c): All spectral ratios of the five events listed in Table 2 (d): Averaged spectral ratio of the five events

in the contents of wave modes, traveling path and arriving direction between microseisms and seismic surface waves, the frequency characteristics of the spectral ratios are nearly same. This means that microseismic observation is very useful for direct

estimation of seismic amplification due to soil deposits.

### 5.3. Stability of spectral ratio for microseisms

For the application of microseisms to seismic microzonation, the stability of spectral ratio should be well examined. One of the sources affecting the reliability is an S/N ratio, in which N means artificial microtremors generated in the urban area plus instrumental noise. As seen in **Fig. 13**, artificial tremors vary with time diurnaly, and are at a minimum level from 2 to 3 o'clock in the morning. Typical instrumental noise spectra are shown in Fig. 18, which are obtained with the same analytical procedure and the same instrumental correction as those of microseisms. The spectral densities in **Fig. 16(a)**, which are from rather calm microseisms in the night, have sufficiently large S/N ratios compared to those in **Fig. 18**. The peak-to-peak amplitudes on the smoked paper at SUM are approximately 0.5–0.7 mm during this time. As seen in **Fig. 1** microseisms with such amplitude level are observed frequently and continuously in winter. In practice it should be known for how long a time we must record microseisms and how many times we must repeat the recording at a given ground site as well as at a standard rock site, simultaneously.

We will examine the reliability with standard deviation. **Fig. 19** shows a relation between moving averaged value (M) and its standard deviation (SD) calculated with N data, ratios of B.P.F. spectra, where N is 3, 4, 6 and 9. We used 90 data in all for 0.63 Hz EW component in the observational period No. 4. The mean of 90 data is 6.9. From this figure we can derive a condition in which SD is significant as a statistiacl measure. In the case of smaller N such as 3 or 4, M often differs

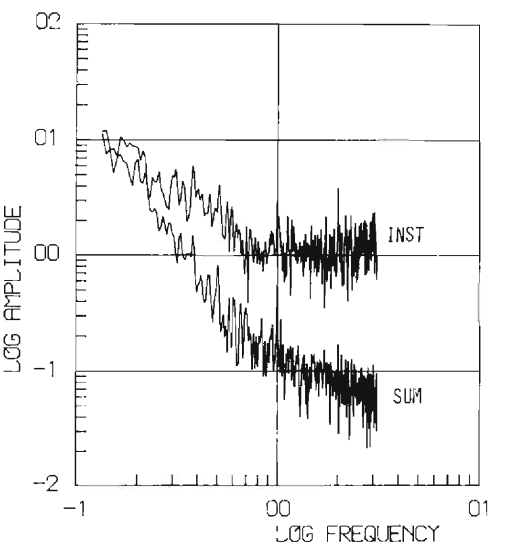


Fig. 18 Fourier spectral densities of typical instrumental noises with an identical analytical procedure to that of microseisms. Amplitude scale is the same as that in Fig. 16 (a), $\mu$ kine sec.

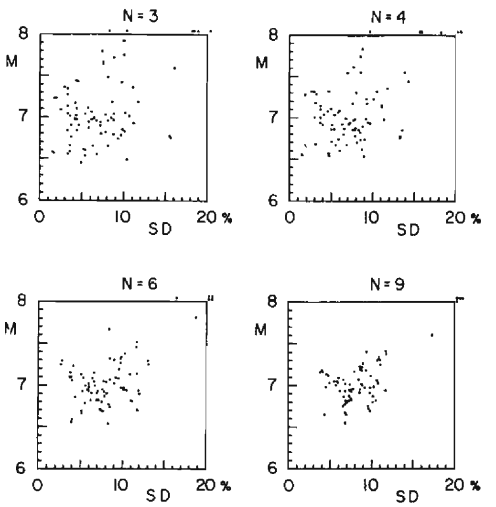


Fig. 19 Relation between moving averaged value (M) and standard deviation (SD) calculated with N ratios of band pass filter amplitudes, (INST/SUM). Note that SD is significant as a statistical measure as long as recordings are repeated at least 6 times at a given ground site and a standard rock site, simultaneously.

from the total mean 6.9 by a large amount even if SD is considered small. In the case of N=6, M is close to 6.9 with a difference of less than 10% as long as SD is less than 15%. Thus, observation with a recording length of longer than 4 minutes should be repeated at least 6 times at different times. It is not preferable to make a recording time longer in return for lessening the number of repeats, in order to save the total time during which an observer must stay at a given observational point. This argument is similar to that in an observation of short period microtremors for seismic microzonation[17].

### 5.4. Geological setting and amplification of microseisms

According to the previous discussion, microseisms should be recorded at least 6 times during the time when the amplitude level of artificial tremors is sufficiently low. Thus simultaneous observations at SUM and temporal sites were carried out more than ten times through the night, to study the effect of site conditions. Locations of the sites are shown in **Fig. 2.**

SHM is located on an outcrop of the Paleozoic strata on the west of the basin. The nature of microseisms at SHM such as spectral shape, amplitude level and temporal variation is identical to that at SUM on the east of the basin. Thus it can be assumed that the same wave group enters into the whole basin as microseisms.

**Fig. 20** shows the results obtained with the B.P.F. analysis. At OGR microseisms could not be recorded accurately because the geophone were blown hard by local wind. The figure shows a result obtained with only one record at the time

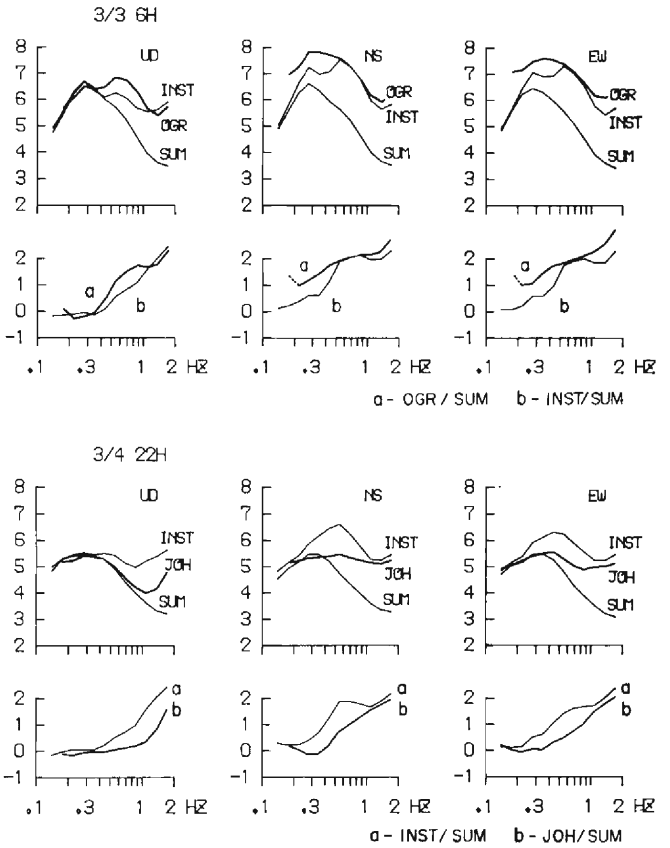


Fig. 20 Characteristics of spectra and spectral ratios of microseisms at different ground sites

when the wind was falling. Thus our discussion can be no more than qualitative.

At OGR, which is located in the center of the southern parts of the basin, amplification of microseisms in the vertical component begins to increase at 0.3–0.4 Hz and has a peak around 0.8 Hz, showing a remarkable contrast to the amplification at GOK (INST) which has no peaks. In the horizontal components there are large amplifications in a wide frequency range of 0.2–0.8 Hz, which include the 0.7 Hz peak amplification at GOK (INST).

The site JOH is located on mountain gravels in the south-eastern part of the basin. As seen in **Fig. 20** the vertical component at JOH has the same amplitude as that at the rock site in the frequency range of lower than 1 Hz. Amplification in each horizontal component begins to increase at 0.4 Hz, which is the highest one in the ground. Amplification at 0.7 Hz is approximately 3 and is smallest in the observations. Thus in the frequency range of lower than 1 Hz the mountain gravels are considered to be the most quake proof deposits in the basin.

From our observations the following results are obtained: amplification due to soil

deposits in the horizontal component begins to increase at lower frequency than that in the vertical one; the horizontal component has larger amplification than the vertical one; a peak frequency of amplification and a critical frequency at which amplification begins to increase become lower as the site moves from the environs to the center of the basin.

According to the calculation of surface wave in irregular soil layers with a finite element model, the energy in the incident fundamental Rayleight mode tends to be transfered to higher modes[7]. As a result interference between modes occurs in soil layers and a spatial variation of amplification is observed according to wave period. This theoretical argument is considered applicable to an interpretation of our observational results.

## 6. Conclusion

Observations of microseisms with periods of longer than 1 second in the Kyoto basin were carried out with monitoring the wave characteristics of incident microseisms at an adjacent outcrop of bedrock to discuss the amplification due to soil deposits and the effects of goelogical setting. The amplification of microseisms was compared with that of the seismic surface waves from near earthquakes. The results including the related problem of seismic microzonation are as follows:

(1). Microseisms with periods of longer than 1 second observed at ground site as well as rock site vary in peak frequency and in peak amplitude according to a meteorological condition and sea waves near Japan. Peak frequency and peak amplitude in spectra of microseisms are not related directly to subsurface structure.

(2). Amplitude of spectral component of microseisms at the ground site varies with time in an identical way to that at the rock site. Parallel variation with time between the two sites is observed in the frequency range lower than about 1 Hz, above which artificial microtremors is predominant with diurnal amplitude variation. The artificial tremors generated in urban area decrease the linear relation between the two sites.

(3). Microseisms at the two rock sites located on the opposite side of the basin are identical in spectral features. It is considered that the same wave group enters into the whole basin as microseisms.

(4). Averaged spectral ratio of microseisms, ground site/rock site, shows a frequency dependent characteristics and is essentially constant with time regardless of their spectral contents. This is considered to show the ground response to microseisms.

(5). Amplification of surface wave due to soil deposits derived with spectral ratio of near earthquakes resembles that of microseisms very well. Averaged spectral ratio of microseisms cover all peaks in the spectral ratios of seismic waves.

(6). Following (3), (4) and (5) seismic amplification can be estimated directly with averaged spectral ratio of microseisms, the reliability of which can be checked with standard deviation as long as the observation with a recording length of longer than 4 minutes is repeated at least 6 times simultaneously at ground and rock sites.

(7). Amplification due to soil deposits in the horizontal component begins to increase at lower frequency than that in the vertical one. The horizontal component has larger amplification than the vertical one.
(8). Peak frequency of amplification and critical frequency at which amplification begins to increase become lower as a site moves from the environs to the center of the basin.

## Acknowledgement

The author wishes to express his sincere thanks to Prof. Soji Yoshikawa of Kyoto University for his encouragement in carrying out this work.

### References

1) Sakajiri N., S. Okada, K. Kudo, S. Naruse, A. Kubotera, F. Takeuchi and T. Mitsunami: Observation of 1– to 5–sec Microtremors and Their Application to Earthquake Engineeering. Part V, Zisin, 2nd Ser., Vol. 31, 1978, pp. 179–193 (in Japanese).
2) Ohta, Y., H. Kagami, N. Goto and K. Kudo: Observation of 1– to 5– Second Microtremors and Their Application to Earthquake Engineering. Part 1., Bull. Seis. Soc. Am., Vol. 68, 1978, pp. 767–779.
3) Kagami, H., C. M. Duke, G. C. Liang and Y. Ohta: Observation of 1– to 5– Second Microtremors and Their Application to Earthquake Engineering. Part II., Bull. Seis. Soc. Am., Vol. 72, 1982, 987–998.
4) Нестеров В.А.: Штормовые Микросейсмы на Острове Шйкотан и Флуктуации Давления Воды на Дне Тихого Океана, Вулканол. и Сейсмол., No. 2, 1982, с. 73–79.
5) Kagami H., J. Horita, Y. Ohta, N. Sakajiri, A. Yoshida, A. Tanaka and A. Kubotera: Observation of 1– to 5–sec Microtremors and Their Application to Earthquake Engineering. Part VIII, Zishin, 2nd Ser., Vol. 36, 1983, pp. 609–617 (in Japanese).
6) Taga N., Y. Togashi, H. Taniguchi and T. Miyazaki: Characteristics of Mictotremors in the Noobi Plain, Proc. Symp. Disaster Sci. 18, 1981, pp. 227 (in Japanese).
7) Drake, L. A.: Love and Rayleigh Waves in an Irregular Soil Layer, Bull. Seis. Soc. Am., Vol. 70, 1980, pp. 571–582.
8) Okano, K.: Observational Study on Microseisms (Part 1), Bull. Disas. Prev. Res. Inst., Kyoto Univ., No. 44, 1961, pp. 2–22.
9) Okano, K.: Observational Study on Microseisms (Part 2), Bull. Disas. Prev. Res. Inst., Kyoto Univ., No. 47, 1961, pp. 2–15.
10) Kitsunezaki C, N. Goto and Y. Iwasaki: Underground Structure of the Southern Part of the Kyoto Basin Obtained from Seismic Explosion and Some Related Problems of Earthquake Engineering, Annuals of Disas. Prev. Res. Inst., Kyoto Univ., No. 14–B, 1971, pp. 203–215 (in Japanese).
11) Akamatsu J. : Observation of Microseisms and Amplification of Surface Waves by Soil Deposits, Annuals of Disas. Prev. Res. Inst., Kyoto Univ. No. 26 B–1, 1983, pp. 43–52 (in Japanese).
12) Akamatsu J.: Seismic Observation at the Sumiyama Seismics Station, Annuals of Disas. Prev. Res. Inst., Kyoto Univ., No. 20 B–1, 1977 pp. 13–19 (in Japanese).
13) Tsuchiya Y., M. Yamaguchi and H. Hiraguchi: Prediction of Ocean Wind Waves with Winter Monsoon in the Japan Sea, Annuals of Disas. Prev. Res. Inst., Kyoto Univ., No. 26 B–2, 1983, pp. 599–635 (in Japanese).
14) Japanese National Committee for Upper Mantle Project: The Crust and Upper Mantle of the Japanese Area Part II, 1973, Geological Survey of Japan, Kawasaki.
15) Akamatsu J., T. Furuzawa and K. Irikura: On Nature of S Waves from Local Small Earthquakes Observed at Amagase Crustal Movement Observatory, Annuals of Disas. Prev. Res. Inst., Kyoto

Univ., No. 18 B, 1975, pp. 11–21 (in Japanese).

16) Akamatsu J. and M. Nishi: On the Seismic Observation with A Symmetrical Three-Components Seismograph System, Annuals of Disas. Prev. Res. Inst., Kyoto Univ., No. 22 B–1, 1979, pp. 83–90 (in Japanese).

17) Ред. Медведева, С. В.: Сейсмическое Микрорайонирование, Наука, 1977, с. 67–75.